Neoplasma 2025; 72(6): 415–429

doi:10.4149/neo_2025_250620N274

HERC1 attenuates gemcitabine resistance of lung cancer cells by inhibiting autophagy through KAT2A ubiquitination

Yanhong WEI, Guanghui TIAN, Zhaohui TANG, Sijuan DING, Zhangwen TANG, Pengfei LUO*

Department of Oncology, The Central Hospital of Yongzhou (Yongzhou Hospital Affiliated to University of South China), Yongzhou City, Hunan Province (Hunan Provincial Demonstration Base for Medical Technology in Tumor Radiotherapy), China.

**Correspondence: lpf1981@yeah.net*

Received June 20, 2025 / Accepted December 4, 2025

Lung cancer, a leading cause of death, is challenging to treat due to gemcitabine resistance. Dysregulated autophagy is associated with chemoresistance. Here, we aimed to study the mechanism of how HERC1 modulates autophagy and gemcitabine sensitivity in lung cancer. Paired tumor and adjacent normal tissues were collected from 30 patients with lung cancer. The viability, proliferation, apoptosis, migratory, and invasive capacity of gemcitabine-resistant A549 and H1299 cells (A549/R and H1299/R) were evaluated using Cell Counting Kit-8 (CCK-8), EdU staining, flow cytometry, wound healing, and Transwell assays, respectively. The interactions among HECT and RLD domain-containing E3 ubiquitin protein ligase family member 1 (HERC1)-lysine acetyltransferase 2A (KAT2A)-phosphatidylinositol-4,5-bisphosphate 3-kinase catalytic subunit beta (PIK3CB) were verified by co-immunoprecipitation. A mouse xenograft tumor model was established. Ki-67 expression was determined by immunohistochemistry. Our data showed that HERC1 expression was downregulated in gemcitabine-resistant tumor tissues and A549/R cells, correlating with poor prognosis. Overexpressing HERC1 suppressed proliferation and migration, enhanced apoptosis in A549/R or H1299/R cells, and simultaneously inhibited autophagy. Mechanistically, HERC1 promoted KAT2A ubiquitination and degradation, which enhanced gemcitabine sensitivity by inhibiting autophagy. Further investigation revealed that KAT2A depletion inhibited the lysine acetylation modification of PIK3CB, leading to inactivation of the PI3K/AKT axis. Additionally, HERC1 suppressed autophagy and gemcitabine resistance in A549/R cells by KAT2A-dependent inactivation of the PI3K/AKT axis. Furthermore, HERC1 overexpression enhanced the inhibition of gemcitabine on tumor growth by suppressing autophagy *in vivo*. In conclusion, HERC1 inhibited autophagy by inactivating PIK3CB-mediated PI3K/AKT signaling via promoting KAT2A degradation, thereby enhancing the gemcitabine sensitivity in lung cancer.

Key words: HERC1; KAT2A; PI3K/AKT; gemcitabine resistance; lung cancer

Lung cancer is the leading cause of global cancer mortality, with 2.4 million cases and 1.8 million deaths annually [1], yet the 5-year survival rate remains below 20% despite treatment advances [2]. Gemcitabine, a cornerstone chemotherapy drug for lung cancer, faces significant limitations due to chemoresistance, which contributes to treatment failure and disease progression [3]. Autophagy functions as a key regulator in the tumor microenvironment and chemoresistance [4]. Notably, pharmacological inhibition of autophagy has been shown to reverse chemoresistance by enhancing apoptotic sensitivity in lung cancer [5], suggesting its therapeutic potential.

HECT and RLD domain-containing E3 ubiquitin protein ligase family member 1 (HERC1), an E3 ubiquitin ligase [6], has recently emerged as a critical regulator of autophagy and chemoresistance in multiple malignancies, including breast cancer [7] and osteosarcoma [8]. Downregulation of HERC1 has been found in lung cancer [9]. However, the functional role of HERC1 in lung cancer chemoresistance remains uncharacterized. Intriguingly, HERC1 mediated the sensitivity to nucleoside analogs in acute myeloid leukemia [10], and its mutations modulated autophagic processes in neurodegenerative diseases [11, 12]. These findings collectively suggest a potential role for HERC1 in autophagy-mediated gemcitabine resistance in lung cancer.

Ubiquitination plays a critical role in regulating protein stability and function in lung cancer [13]. Bioinformatic analyses predict that HERC1 acts as an E3 ligase for lysine acetyltransferase 2A (KAT2A), which is involved in cancer progression and partially promotes splicing factor 3b subunit 4 (SF3B4)-driven tumorigenesis in lung cancer [14, 15]. Thus, we hypothesize that HERC1 modulates autophagy and

gemcitabine sensitivity in lung cancer cells via regulating KAT2A ubiquitination.

PI3K/AKT signaling is known to exacerbate gemcitabine resistance in lung cancer [16, 17]. The PI3K/AKT axis is linked with autophagy regulation in multiple tumors [18], and blocking PI3K/AKT signaling suppressed chemoresistance in lung cancer [19, 20]. Additionally, phosphatidylinositol-4,5-bisphosphate 3-kinase catalytic subunit beta (PIK3CB), a catalytic subunit of PI3K [21], plays a crucial role in this process [22]. Importantly, bioinformatics predictions also identify lysine acetylation modification sites in PIK3CB.

In conclusion, we supposed that HERC1 decreased KAT2A by promoting its ubiquitination and degradation. The downregulation of KAT2A inhibited lysine acetylation of PIK3CB, leading to the inactivation of the PI3K/AKT signaling, which suppressed autophagy and enhanced the sensitivity to gemcitabine, ultimately inhibiting the malignancy of lung cancer.

Materials and methods

Data sources and clinical tissue samples. The expression of HERC1 in normal tissues and tumor tissues of LUAD and LUSC was obtained from GEPIA (http://gepia.cancer-pku.cn/) [23]. The KAT2A expression in normal tissues and tumor tissues of LUAD and LUSC was collected from TIMER (https://cistrome.shinyapps.io/timer/) [24]. Prognostic outcomes for lung cancer patients with differential expression of HERC1 and KAT2A were also estimated by Kaplan-Meier analysis (https://kmplot.com/analysis/) as previously described [25]. Additionally, 30 pairs of cancerous and normal tissues were collected from lung cancer patients at Yongzhou Central Hospital. These included 13 cases identified as gemcitabine-resistant (resistance) and 17 cases with gemcitabine-sensitive tissues (sensitive). The clinical information for patients enrolled in this study is shown in Supplementary Table S1.

Cell culture and transfection. 293T cells, A549 cells, and H1299 cells (ATCC, USA) were used. To establish gemcitabine-resistant lung cancer cells (A549/R and H1299/R), A549 and H1299 cells were exposed to a low-dose gemcitabine mixed medium as previously described [26]. The cells were cultured in RPMI-1640 medium (Thermo Scientific HyClone, USA), containing 10% FBS (Gibco, USA), 100 U penicillin, and 100 μg/ml streptomycin at 37 °C and 5% CO_2.

Cell transfection. For the construction of the HERC1 or KAT2A overexpression plasmid, the full-length sequences of HERC1 and KAT2A were cloned into the pcDNA3.1 vector. For HERC1 and KAT2A knockdown, short hairpin RNA (shRNA) targeting HERC1 (sh-HERC1) or KAT2A (sh-KAT2A) was synthesized. The shRNA sequences used for knockdown are as follows: sh-HERC1: GCTGATAAACTGAGTCCCAAA; sh-KAT2A: GCTGAACTTTGTGCAGTACAA. These plasmids and the stable overexpression of the HERC1 plasmid were synthesized by GenePharma (Shanghai, China). The above plasmids were transfected into cells using Lipo6000 reagent (Beyotime, Shanghai, China), and incubation lasted for 48 h.

***In vivo* xenograft tumor model.** BALB/c nude mice (4–6 weeks old, 18–22 g) were obtained from Beijing SPF (China) and housed at 24–26 °C with 50–70% humidity, a 12-h light/dark cycle, and free access to food and water. The mice were randomized into four groups: oe-NC, oe-HERC1, GEM, and GEM+oe-HERC1. A549 cells (1×10^7) stably expressing oe-NC or oe-HERC1 were subcutaneously implanted into the right flank of the mice. Two weeks after injection, the mice in the GEM group and the GEM+oe-HERC1 group were intraperitoneally administered 50 mg/kg/day gemcitabine every three days. Tumor size was measured using calipers. One month post-transplantation, mice were euthanized with CO_2, and tumors were excised, weighed, and analyzed histologically. All experimental protocols were approved by the Institutional Animal Care and Use Committees of the University of South China Laboratory Animal Center.

Immunohistochemistry (IHC). The paraffin tumor sections were first deparaffinized using ethanol. Following rehydration with 3% hydrogen peroxide (H_2O_2), the slides were incubated overnight at 4 °C with the primary antibody Ki-67 (#ab16667, 1:200). The next day, the sections were treated with the goat anti-rabbit IgG H&L (HRP) preadsorbed (#ab7090, 1:200, Abcam) at 37 °C for 30 min. Subsequently, the sections were stained with diaminobenzidine (DAB) and examined under a microscope.

Quantitative reverse transcription polymerase chain reaction (qRT-PCR). Total RNA was extracted using Trizol reagent (Invitrogen, USA), and 1 μg RNA was reverse transcribed into cDNA using a Prime-Script™ one-step qRT-PCR kit (Takara Bio, China). qPCR was performed on an ABI7900 Real-Time PCR System (Applied Biosystems, USA). The mRNA expression was normalized to glyceraldehyde-3-phosphate dehydrogenase (GAPDH), and calculated using the $2^{-\Delta\Delta CT}$ method. Primers sequences used were as follows: HERC1 forward 5'-AGCTGAAATGGCTTGAACACT-3', HERC1 reverse 5'-GCAACTCCCTCTCTTGTAGCA-3'; KAT2A forward 5'-GCAAGGCCAATGAAACCTGTA-3', KAT2A reverse 5'-TCCAAGTGGGATACGTGGTCA-3'; PIK3CB forward 5'-TATTTGGACTTTGCGACAAGACT-3', PIK3CB reverse 5'-TCGAACGTACTGGTCTGGATAG-3'; GAPDH forward 5'-GGAGCGAGATCCCTCCAAAAT-3', GAPDH reverse 5'-GGCTGTTGTCATACTTCTCATGG-3'.

Western blot. Proteins from tumor tissues, xenograft tumors, and cultured cells were extracted using radioimmunoprecipitation assay (RIPA) buffer (#20188, Sigma-Aldrich, USA) and quantified by a bicinchoninic acid (BCA) Protein Assay Kit (Beyotime, China). The samples underwent electrophoretic resolution via sodium dodecyl sulfate polyacrylamide gel electrophoresis (SDS-PAGE) followed by semi-dry transfer to polyvinylidene fluoride (PVDF)

membranes. Following this, the membrane was blocked with 5% bovine serum albumin (BSA), and the primary antibody was incubated overnight at 4 °C. After washing, the membranes were incubated with secondary antibodies (#ab7090, Abcam) at 37 °C for 45 min. Protein band images were taken, and quantitative densitometry analysis was conducted by Image-Pro Plus software (Media Cybernetics, Inc., USA). Primary antibodies used were: HERC1 antibody (#MBS9145890, 1:500, Mybiosource, https://www.mybiosource.com), KAT2A antibody (#MBS6005990, 1:500, Mybiosource), PIK3CB antibody (#MBS620204, 0.1 μg/ml, Mybiosource), Bax antibody (#MBS9600058, 1/500, Mybiosource), Cleaved Caspase-3 (C-caspase3) antibody (#MBS631626, 1:1000, Mybiosource), Bcl-2 antibody (#MBS2085983, 0.5 μg/ml, Mybiosource), LC3II/I antibody (#MBS616452, 1:100, Mybiosource), Beclin1 antibody (#MBS9610748, 1:500, Mybiosource), p62 antibody (#MBS244060, 1.0 μg/ml, Mybiosource), PI3K antibody (#4292S, 1:1000, Cell Signaling Technology), p-PI3K (#4228T, 1:1000, Cell Signaling Technology), AKT antibody (#9272S, 1:1000, Cell Signaling Technology), p-AKT antibody (#4060S, 1:2000, Cell Signaling Technology), and GAPDH antibody (#2118, 1:1000, Cell Signaling Technology).

Protein stability assay. The protein stability of KAT2A and PIK3CB was evaluated using a proteasome inhibition assay with MG132 and a cycloheximide (CHX) chase assay. After transfection of the HERC1 overexpression plasmid or the NC plasmid, cells were treated with 5 μM proteasome inhibitor MG132 for 6 h to inhibit proteasomal degradation. Additionally, cells were treated with 100 μM CHX for varying time points (0, 3, 6, and 9 h) following the overexpression of HERC1 or KAT2A to block protein synthesis. Following treatment, cell lysates were collected, and protein expression of KAT2A and PIK3CB was analyzed by immunoblotting.

Cell Counting Kit-8 (CCK-8) and EdU staining. Cells (1.0×10^4) were seeded into 96-well plates and incubated for 24, 48, 72, and 96 h. Afterwards, the cells were treated with 10 μl of CCK-8 solution (Sigma-Aldrich, USA) and incubated at 37 °C for an additional hour. The optical density of the solutions at 450 nm was measured using a scanning microplate reader (Bio-Rad, USA). A549/R cells were exposed to gemcitabine (0.1, 1, 10, 100, 1000 μM) for 48 h, and the half-maximal inhibitory concentration (IC_{50}) value was determined by GraphPad Prism with nonlinear regression analysis.

Cell proliferation was evaluated using the EdU staining assay. After incubation with 50 μM EdU buffer, fixation with 4% formaldehyde, and permeabilization with 0.1% Triton X-100, the samples were supplemented with EdU solution, followed by Hoechst staining of the nuclei. Finally, samples were examined using a fluorescence microscope.

Wound healing assay. Following 48 h of transfection, cells were plated in a 6-well plate. A scratch was created in the cell layer using a 200 μl sterile pipette tip, generating a wound in the well. Pictures of the wound were taken at 0 h (immediately after scratching) and after 24 h of culture to monitor the gap closure. Images were evaluated by the ImageJ software (NIH, USA).

Transwell assay. The invasive capability of A549/R and H1299 cells was assessed using 24-well Transwell chambers. Cells (2.5×10^4 cells/100 μl) were resuspended in serum-free medium supplemented with 1% BSA (Sigma-Aldrich) and placed in the top chamber, precoated with 100 μl diluted substrate gel (Sigma, USA). 500 μl of Dulbecco's modified Eagle medium (DMEM) containing 10% FBS was then introduced into the lower chamber. Following a 24 h incubation, the samples were stained with 0.1% crystal violet, and the invasive cells were quantified using a microscope.

Flow cytometry. After transfection, the cell apoptosis was evaluated using a flow cytometry assay. The cells were collected, washed with PBS, and labeled with Annexin V-FITC (BD Biosciences) and PI (Sigma-Aldrich) in binding buffer (BD Biosciences) for 15 min, avoiding exposure to light. Cells were determined on a BD FACSCalibur flow cytometer (BD Biosciences). Apoptosis was quantified using FlowJo software (FlowJo LLC).

Co-immunoprecipitation (co-IP). The interaction between KAT2A and HERC1 or PIK3CB was investigated by co-IP. Following cell lysis in RIPA buffer (#P0013D, Beyotime, China), samples were incubated overnight at 4 °C with either anti-HERC1 (#MBS3902336, 6 μg/mg lysate, Mybiosource) antibody, anti-KAT2A antibody (#MBS388597, 10 μl per IP, Mybiosource), or anti-PIK3CB antibody (#MBS8542640, 1:100, Mybiosource), with IgG as the control. Antibody-protein complexes were bound to protein A/G magnetic beads for 2 hours, followed by washing with ice-cold lysis buffer three times. Reciprocal interactions were detected by immunoblotting with antibodies against HERC1, KAT2A, or PIK3CB.

Identification of ubiquitination. To assess ubiquitination of KAT2A, A549/R cells were transfected with either HERC1 overexpressing plasmids or control plasmids with proteasome inhibitor MG132 (5 μM). After transfection, samples were lysed in RIPA buffer with protease and deubiquitinase inhibitors. For immunoprecipitation (IP), lysates were immunoprecipitated with anti-KAT2A antibody (#MBS388597, 10 μl per IP, Mybiosource) overnight at 4 °C, followed by protein A/G bead pulldown and stringent washing. Ubiquitinated KAT2A levels were detected by western blot using anti-ubiquitin antibody (Ub, #MBS2125129, 1:500, Mybiosource) and anti-KAT2A antibody (#MBS6005990, 1:500, Mybiosource).

Identification of acetylation. To evaluate acetylation of PIK3CB, 293T cells were transfected with vector, HA-PIK3CB, Myc-KAT2A + HA-PIK3CB, or sh-KAT2A-Myc + HA-PIK3CB. After 48 h, cells were lysed in RIPA buffer with deacetylase inhibitors. HA-tagged PIK3CB was precipitated from cell lysates using anti-HA-agarose antibody (#A2095, 1:100, Sigma Aldrich) overnight at 4 °C, followed by protein A/G bead capture. After washing three times, acetylation was evaluated by immunoblotting with anti-acetyl-lysine

antibody (ACK, #9441, 1:100, Cell Signaling Technology), anti-HA antibody (#3724, 1:1000, Cell Signaling Technology) for IP validation, and Myc-Tag (#71D10) rabbit mAb (#2272, 1:1000, Cell Signaling Technology) to detect KAT2A expression.

Immunofluorescence staining. LC3B expression and cellular localization of KAT2A and PIK3CB were detected by immunofluorescence staining. Cells were fixed with 4% paraformaldehyde, permeabilized with 0.2% Triton X-100, and then blocked with 10% goat serum for 2 hours. Subsequently, the samples were incubated with primary antibodies specific to KAT2A (#MBS8572528, 1:50, Mybiosource) and PIK3CB (#MBS9407711, 1:100, Mybiosource) or LC3B antibody (#MBS616452, 1:100, Mybiosource) overnight at 4 °C. The cells were then exposed to a secondary antibody (#MBS688397, 1 mg/ml, Mybiosource) at room temperature for 1 h. After labeling the nuclei with 4',6-diamidino-2-phenylindole (DAPI, Sigma Aldrich, USA), the slices were visualized using a laser scanning confocal microscope (Olympus CX23, Japan).

Data analysis. Statistical analyses were conducted using SPSS (version 27, IBM, USA). Data are presented as mean ± standard deviation (SD). For comparisons between two groups, Student's t-test was used. For comparisons among three or more groups, one-way analysis of variance (ANOVA) followed by Tukey's tests was applied. The correlation between KAT2A and HERC1 or PIK3CB was assessed by Spearman's correlation coefficient. A p-value <0.05 was defined as statistically significant. All experiments were performed in three independent biological replicates, each performed in triplicate.

Results

HERC1 expression was downregulated in lung cancer. The GEPIA database showed that HERC1 was significantly downregulated in lung cancer tissues (Figure 1A). Furthermore, the low expression of HERC1 was associated with a poor prognosis (Figure 1B). To further validate these findings, HERC1 expression was analyzed. As expected, the expression level of HERC1 was decreased in the tumor group (Figures 1C, 1D). Additionally, HERC1 expression was assessed in cancer samples from 13 gemcitabine-resistant patients (resistance) and 17 gemcitabine-sensitive patients, respectively. Compared to gemcitabine-sensitive tissues, HERC1 expression was obviously reduced in gemcitabine-resistant tissues (Figure 1E). Similarly, HERC1 expression was markedly lower in gemcitabine-resistant A549 cells (A549/R) than in gemcitabine-sensitive A549 cells (A549) (Figures 1F, 1G). These findings indicated that HERC1 expression was decreased in lung cancer, particularly in gemcitabine-resistant A549 cells.

HERC1 overexpression inhibited autophagy and proliferation of gemcitabine-resistant A549 and H1299 cells. To explore whether HERC1 affects gemcitabine resistance in lung cancer, we transfected A549/R cells with plasmids overexpressing HERC1. We observed that HERC1 was successfully overexpressed in A549/R cells (Figures 2A, 2B). To evaluate the IC_{50} of each group, A549/R cells were treated with varying doses of gemcitabine (0.1, 1, 10, 100, 1000 μM). The results revealed that the IC_{50} of the oe-HERC1 group was lower than that of the NC group (49.5 μM vs. 105.9 μM) (Figure 2C). Furthermore, overexpression of HERC1 suppressed the viability of A549/R cells (Figure 2D). EdU staining further confirmed that the HERC1 upregulation exhibited an inhibitory effect on the proliferation of A549/R cells (Figure 2E). Furthermore, increased HERC1 expression notably suppressed the migration and invasion of A549/R cells (Figure 2F, 2G). Compared to the NC group, HERC1 overexpression accelerated cell apoptosis (Figure 2H). Consistent with this, a marked elevation in C-caspase3 and Bax proteins, along with a reduction in Bcl-2 protein, was observed in the oe-HERC1 group (Figure 2I). Next, we assessed the impact of HERC1 on autophagy in A549/R cells. Figure 2J demonstrated that the upregulation of HERC1 reduced the number of LC3B in A549/R cells transfected with overexpressing HERC1 compared to the NC group. Similarly, a significant reduction in LC3II/I and Beclin1 proteins, along with an enhancement in p62 protein, was found in the oe-HERC1 group (Figure 2K). H1299/R cells were used to validate the role of HERC1 in autophagy and gemcitabine resistance. HERC1 expression was significantly upregulated in the oe-HERC1 group (Supplementary Figures S1A, S1B). H1299/R cells were exposed to gemcitabine at the concentrations of 0.1, 1, 10, 100, and 1000 μM. As expected, the oe-HERC1 group showed lower IC50 than the NC group, and overexpressing HERC1 reduced cell proliferation (Supplementary Figures S1C, S1D). Furthermore, upregulation of HERC1 repressed the migration and invasion of H1299/R cells (Supplementary Figures S1E, S1F) and promoted their apoptosis (Supplementary Figures S1G, S1H). Moreover, increased HERC1 led to significant suppression of cell autophagy (Supplementary Figures S1I, S1J). Additionally, the regulation of HERC1 on autophagy in parental A549 and H1299 cells was also examined. As shown in Supplementary Figure S2, HERC1 overexpression significantly decreased LC3II/I and Beclin1 expression, while promoting p62 expression, in A549 and H1299 parental cells. Overall, upregulating HERC1 suppressed autophagy and proliferation in gemcitabine-resistant lung cancer cells.

HERC1 promoted ubiquitination and degradation of KAT2A. To elucidate the downstream effector of HERC1 in lung cancer, we focused on KAT2A, a histone acetyltransferase implicated in autophagy regulation. TIMER database analysis indicated obvious KAT2A elevation in lung cancer tissues, and lower expression of KAT2A correlates with a better prognosis (Figures 3A, 3B). To further validate KAT2A expression, we conducted qRT-PCR and western blot to assess its levels in tumor samples and normal tissues from lung cancer patients. Consistent with bioinformatics predic-

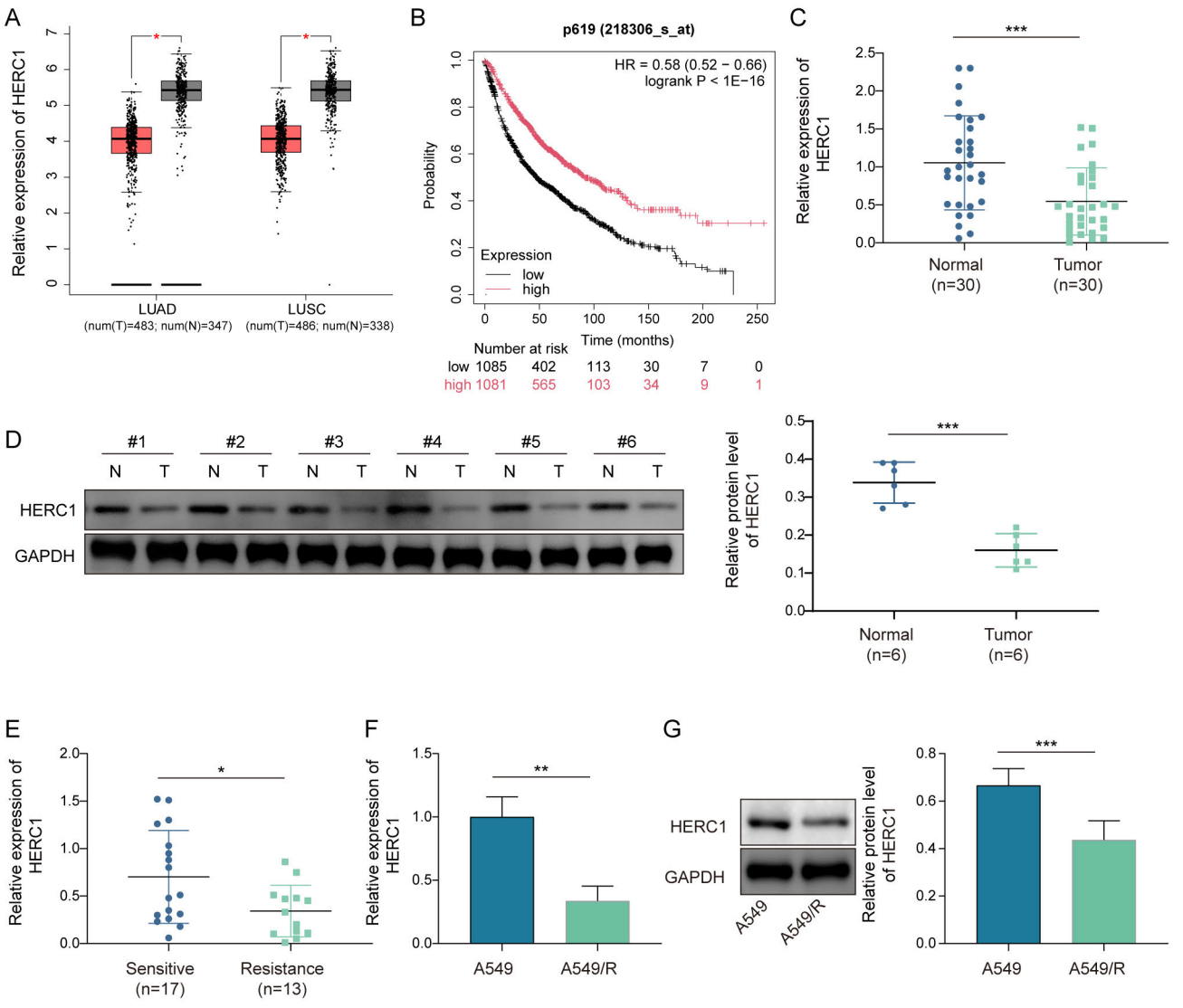

Figure 1. HERC1 expression was downregulated in lung cancer. A) GEPIA database predicted the expression of HERC1 in lung cancer tissues and normal tissues. B) Kaplan-Meier survival analysis estimated the survival of lung cancer patients with high HERC1 expression and low HERC1 expression. C) Tumor tissue and normal tissue of 30 patients with lung cancer were collected. The level of HERC1 in tissues was determined by qRT-PCR (n=30). D) Western blot was conducted to assess the protein expression levels of HERC1 in human lung cancer tissues and their corresponding adjacent non-tumor tissues (n=6). E) HERC1 expression in cancer samples from patients resistant to gemcitabine (resistance, n=13) and patients sensitive to gemcitabine (sensitive, n=17) was determined by qRT-PCR. F) HERC1 expression in A549 and A549/R was detected by qRT-PCR (n=3). G) HERC1 expression was assessed by western blot (n=3). Data were expressed as mean ± SD. *p<0.05, **p<0.01, ***p<0.001

tions, KAT2A was significantly increased in lung cancer tissues (Figures 3C, 3D). Notably, we observed a negative correlation between HERC1 and KAT2A (Figure 3E). Additionally, KAT2A expression was higher in gemcitabine-resistant tissue than in gemcitabine-sensitive tissues (Figure 3F). These findings led us to hypothesize a regulatory interaction between HERC1 and KAT2A in lung cancer. First, the modification types of KAT2A were explored using the PhosphositePlus database (https://www.phosphosite.org/homeAction) (Figure 3G). We then examined whether HERC1 regulated KAT2A stability through ubiquitination. Overexpression of HERC1 resulted in a reduction in KAT2A levels. However, HERC1-induced inhibition of KAT2A was blocked when the proteasome inhibitor MG132 was applied (Figure 3H). Cycloheximide chase assays revealed accelerated KAT2A degradation in HERC1-overexpressing A549/R cells (Figure 3I). To identify the directional regulation of HERC1 on KAT2A, a co-IP assay was performed. Compared to the IgG control group, the HERC1 antibody significantly enriched KAT2A. Similarly, KAT2A antibody selec-

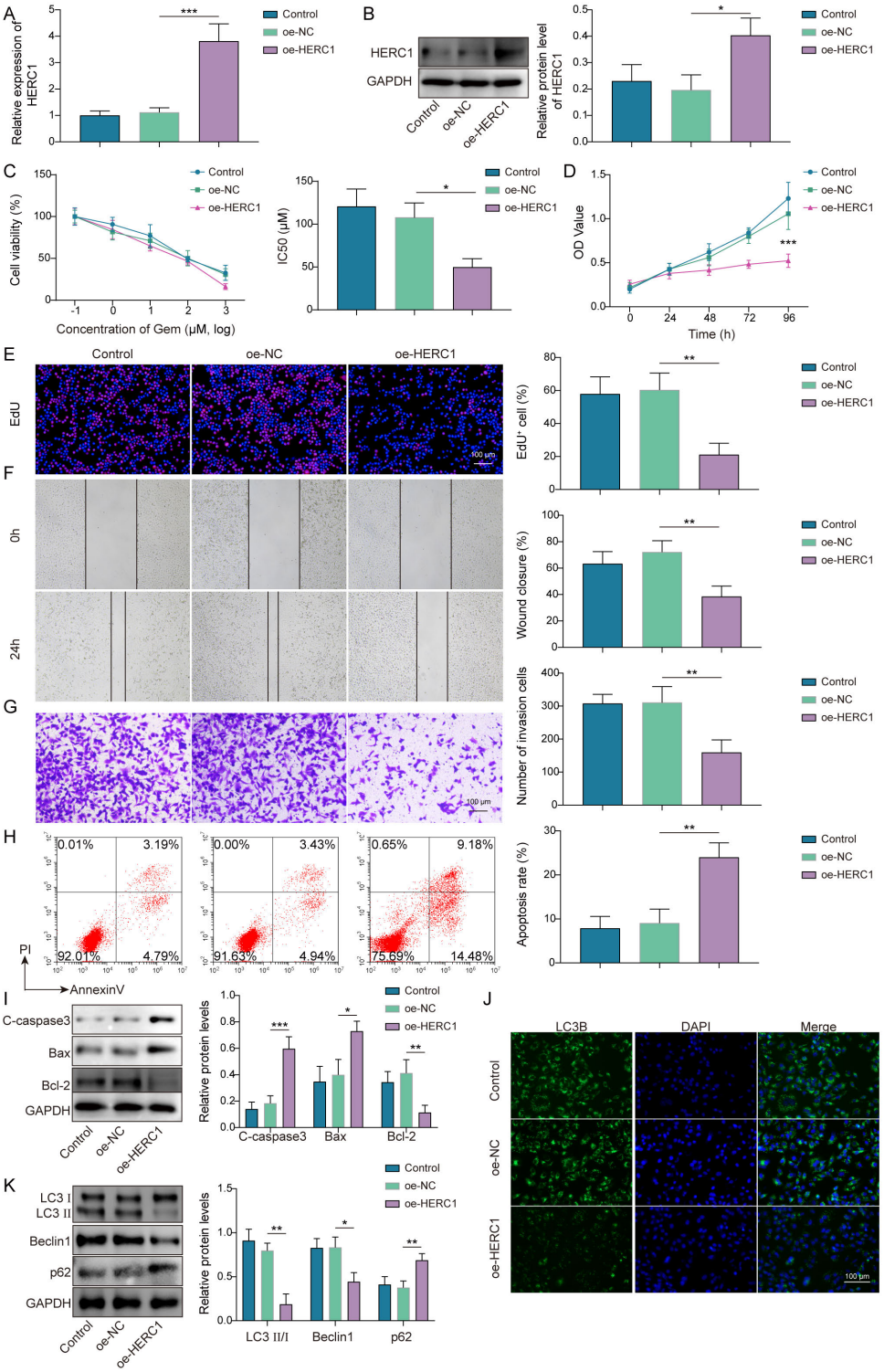

Figure 2. HERC1 overexpression inhibited autophagy and proliferation of gemcitabine-resistant A549 cells. A) A549/R cells were transfected with overexpressing HERC1 or a negative control. qRT-PCR assay was conducted to calculate HERC1 expression in A549/R cells. B) HERC1 protein expression was quantified using western blot. C) A549/R cells were treated with gemcitabine at different concentrations (0.1, 1, 10, 100, 1000 μM). Cell viability was evaluated by the CCK-8 assay. A549/R cells were treated with oe-HERC1. D) Cell viability was assessed by CCK-8 assay. (E) Cell proliferation was evaluated by EdU staining. F) Wound healing assay was applied to assess the migratory ability of cells. G) Transwell assay was performed to assess the invasive ability of cells. H) Cell apoptosis rate was detected by flow cytometry. I) Protein levels of C-caspase3, Bax, and Bcl-2 were examined by western blot. J) The expression level of LC3B was detected by immunofluorescence. (K) LC3II/I, Beclin1, and p62 were quantified by western blot, n=3. Data were expressed as mean ± SD. *p<0.05, **p<0.01, ***p<0.001

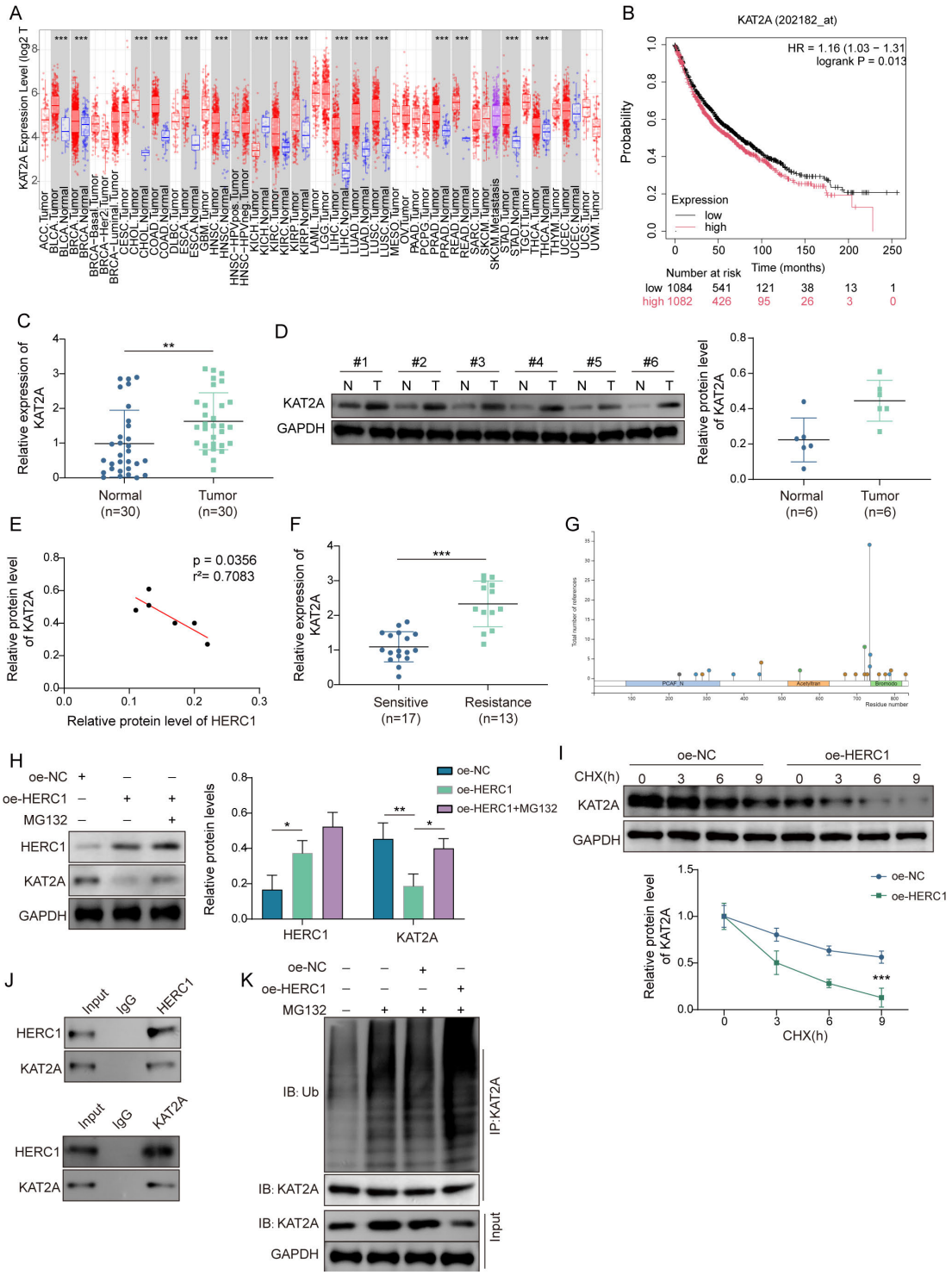

Figure 3. HERC1 promoted ubiquitination and degradation of KAT2A. A) TIMER database analysis predicted KAT2A expression in lung cancer tissues and normal tissues. B) Kaplan-Meier curve estimated the survival of lung cancer patients with high KAT2A expression and low KAT2A expression. C) qRT-PCR was used to detect KAT2A expression in tumor samples and normal tissues of 30 patients with lung cancer. D) Western blot was conducted to assess the protein expression levels of KAT2A in tumor samples and normal tissues (n=6). E) A correlation between HERC1 and KAT2A expression was identified by Pearson's correlation analysis. F) KAT2A expression in cancer samples of patients resistant to gemcitabine (n=13) and patients sensitive to gemcitabine (n=17) was determined by qRT-PCR. G) The modification types of KAT2A were identified by using the PhosphositePlus database. H) Western blot was used to determine the protein levels of HERC1 and KAT2A. I) After CHX treatment for 0, 3, 6, or 9 h, KAT2A protein level was evaluated via western blotting. J) The interaction between HERC1 and KAT2A was verified by co-IP assay. K) The ubiquitination level of KAT2A in A549/R cells was determined using co-IP, n=3. Data were expressed as mean ± SD. *p<0.05, **p<0.01, ***p<0.001

tively pulled down HERC1 in A549/R cells (Figure 3J), and the elevation of HERC1 enhanced KAT2A ubiquitination (Figure 3K). Collectively, these data illustrated that HERC1 reduced KAT2A expression by promoting its ubiquitination and degradation.

HERC1 enhanced gemcitabine sensitivity by inhibiting autophagy via promoting KAT2A degradation in gemcitabine-resistant A549 cells. To explore the functional mechanism of the HERC1/KAT2A axis in modulating autophagy and gemcitabine resistance, A549/R cells were transfected with plasmids overexpressing HERC1 or KAT2A. We observed effective upregulation of KAT2A in A549/R cells (Figures 4A, 4B). Overexpressing HERC1 inhibited cell proliferation, which was reversed by KAT2A overexpression (Figures 4C, 4D). Similarly, KAT2A upregulation abolished HERC1-mediated suppression of migration and invasion (Figures 4E, 4F). Additionally, overexpression of KAT2A reversed the oe-HERC1-induced promoting effect on cell apoptosis (Figure 4G). Consistently, HERC1 increased C-caspase3 and Bax while reducing Bcl-2, with KAT2A co-expression reversing these effects (Figure 4H). As shown in Figure 4I, upregulating HERC1 reduced the fluorescence intensity of LC3B, which was rescued by KAT2A overexpression. Additionally, the increase in HERC1 expression decreased the LC3II/I and Beclin1 expression, while promoting p62 accumulation. However, overexpression of KAT2A reversed these effects of HERC1 on autophagy-related proteins (Figure 4J). Taken together, HERC1 enhanced gemcitabine sensitivity in A549/R by promoting KAT2A degradation and suppressing autophagy.

KAT2A activated PI3K/AKT signaling axis by mediating the lysine acetylation of PIK3CB. Emerging evidence suggests that PI3K/AKT signaling is involved in cell autophagy, and PIK3CB enhances AKT phosphorylation, leading to activation of the PI3K/AKT pathway [27]. Thus, we explored the role and underlying regulating mechanism of PIK3CB in lung cancer. PIK3CB was found to be evidently upregulated in tumor samples compared to adjacent normal tissues collected from patients with lung cancer (Figures 5A, 5B). Significantly, a positive correlation was observed between KAT2A and PIK3CB (Figure 5C). In addition, Myc-KAT2A significantly enhanced the lysine acetylation of PIK3CB (Figure 5D). Co-IP assay further validated the interaction between KAT2A and PIK3CB (Figure 5E). Furthermore, KAT2A and PIK3CB were co-localized in both the nucleus and cytoplasm of A549/R cells (Figure 5F). To further study the mechanism by which KAT2A enhances the lysine acetylation of PIK3CB, we constructed point mutation plasmids targeting acetylation sites K44 and K460. The results indicated that both K44 and K460 mutants remarkably decreased the acetylation levels in 293T cells transfected with Myc-KAT2A (Figure 5G). The depletion of KAT2A inhibited the acetylation of PIK3CB, while overexpression of KAT2A enhanced its acetylation (Figure 5H). After treatment with CHX, KAT2A upregulation heightened the stability of PIK3CB protein (Figure 5I). In addition, the elevation of KAT2A activated PI3K/AKT signaling through increasing PI3K and AKT phosphorylation (Figure 5J). In conclusion, these findings supported that overexpressing KAT2A activated the PI3K/AKT signaling pathway via mediating the lysine acetylation of PIK3CB.

HERC1 suppressed autophagy and proliferation of gemcitabine-resistant A549 cells by inactivating the PI3K/AKT signaling axis through KAT2A. To further verify the functional mechanism of HERC1/KAT2A-mediated PI3K/AKT pathway on autophagy and proliferation of gemcitabine-resistant cells, A549/R cells were transfected with sh-KAT2A with or without sh-HERC1, or treated with PI3K activator 740 Y-P. Compared to the sh-NC group, knockdown of KAT2A significantly suppressed the proliferation of A549/R. However, knockdown of HERC1 or treatment with 740 Y-P mitigated the suppressive effect of KAT2A on proliferation (Figure 6A). These results were supported by EdU staining (Figure 6B). It also showed that silencing of KAT2A markedly reduced migration and invasion of cells, which was reversed by co-silencing of HERC1 or 740 Y-P treatment (Figures 6C, 6D). As shown in Figure 6E, HERC1 depletion or 740 Y-P intervention diminished the pro-apoptotic effect induced by sh-KAT2A on A549/R cells. Consistently, the downregulation of KAT2A promoted the expression of C-caspase3 and Bax, while reducing Bcl-2 levels. Conversely, HERC1 silencing or 740 Y-P treatment counteracted the regulatory effects of sh-KAT2A on apoptosis-related proteins (Figure 6F). These findings illustrate that HERC1 restrains the growth of A549/R cells by suppressing the KAT2A-mediated PI3K/AKT axis. Next, the regulating mechanism of HERC1 on cell autophagy was explored. Autophagy analysis demonstrated that KAT2A suppressed LC3B expression (Figure 6G). Besides, silencing of KAT2A suppressed LC3II/I and Beclin1 expression but increased p62 accumulation. In contrast, co-silencing of HERC1 or 740 Y-P intervention reversed the regulatory effects of KAT2A on autophagy-related proteins (Figure 6H). Furthermore, the suppressive impacts of sh-KAT2A on PI3K/AKT phosphorylation were significantly rescued by either HERC1 depletion or 740 Y-P treatment in A549/R cells, thereby reversing sh-KAT2A-mediated PI3K/AKT inhibition (Figure 6I). Overall, HERC1 suppressed proliferation and autophagy in gemcitabine-resistant A549 cells by the inactivation of PI3K/AKT via KAT2A ubiquitination.

HERC1 overexpression enhanced gemcitabine sensitivity by suppressing autophagy in the xenograft tumor model. The role and its regulating mechanism of HERC1 in gemcitabine resistance were studied *in vivo*. A mouse xenograft tumor model was established by subcutaneous transplantation of A549 cells transfected with stable oe-HERC1 or oe-NC. Gemcitabine treatment or HERC1 overexpression reduced tumor volume and weight in mouse models. The combination of gemcitabine treatment and HERC1 overexpression resulted in a further significant decrease in tumor volume and weight compared with

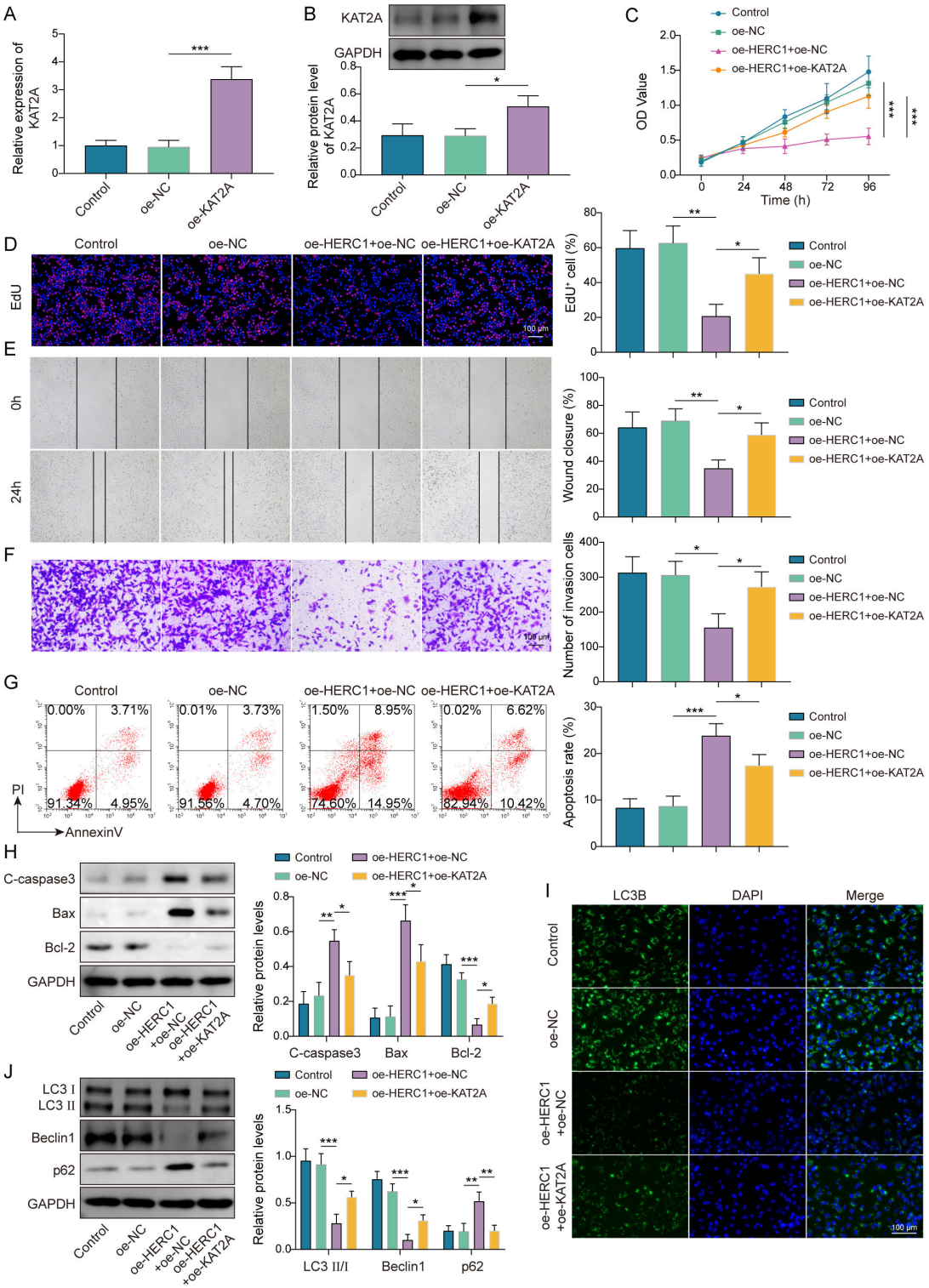

Figure 4. HERC1 enhanced gemcitabine sensitivity by inhibiting autophagy via promoting KAT2A degradation. A, B) qRT-PCR and western blot were used to detect KAT2A expression in A549/R cells transfected with KAT2A overexpression. A549/R cells were transfected with overexpressing HERC1 with/without overexpressing KAT2A. C, D) Cell viability and proliferation were evaluated by CCK-8 and EdU staining. E) Wound healing assay was performed to assess the migratory ability of cells. F) Transwell assay was performed to assess the invasive ability of cells. G) The number of apoptotic cells was quantified using flow cytometry. H) Protein levels of C-caspase3, Bax, and Bcl-2 were evaluated by western blot. I) The expression of LC3B was assessed by immunofluorescence. J) LC3II/I, Beclin1, and p62 were quantified by western blot, n=3. Data were expressed as mean ± SD. *p<0.05, **p<0.01, ***p<0.001

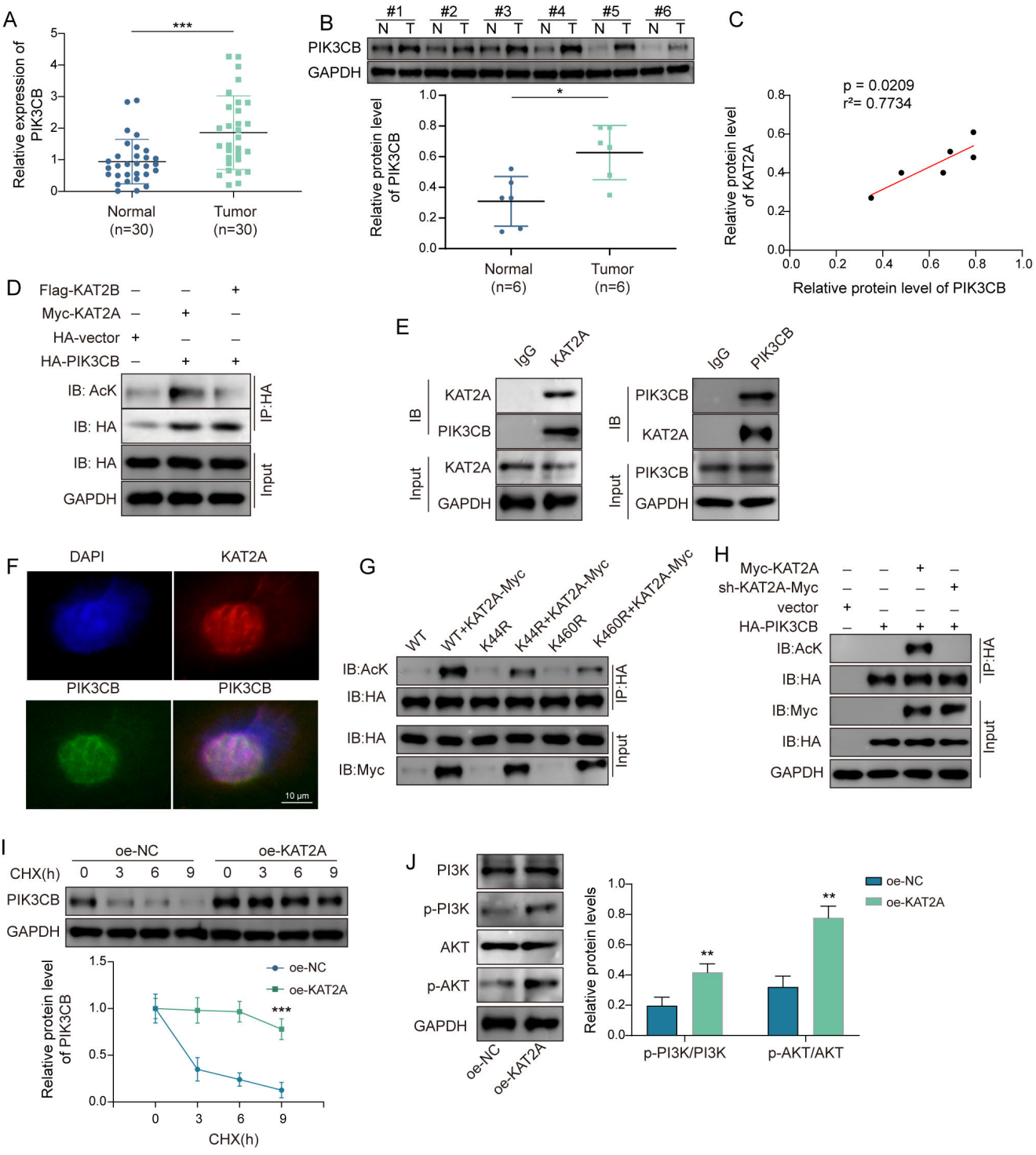

Figure 5. KAT2A activated PI3K/AKT signaling axis by mediating the lysine acetylation of PIK3CB. A) qRT-PCR was used to detect PIK3CB expression in tumor tissues and normal tissues of 30 patients with lung cancer (n=30). B) Western blot was conducted to assess the protein expression of PIK3CB in tumor samples and normal tissues (n=6). C) A correlation between PIK3CB and KAT2A expression. D) PIK3CB acetylation modification was analyzed by co-IP assay. E) The interaction between KAT2A and PIK3CB was validated by co-IP assay. F) The localization of KAT2A and PIK3CB in A549/R cells was detected using immunofluorescence. G) A549/R cells were transfected with wild-type or mutant PIK3CB and KAT2A overexpression. The acetylation level was examined using a co-IP assay. H) Co-IP assay was conducted to examine the acetylation level of PIK3CB in A549/R cells. I) After CHX treatment for 0, 3, 6, or 9 h, PIK3CB expression was evaluated via western blot. J) The phosphorylation levels of PI3K and AKT were assessed using western blot, n=3. Data were expressed as mean ± SD. *p<0.05, **p<0.01, ***p<0.001

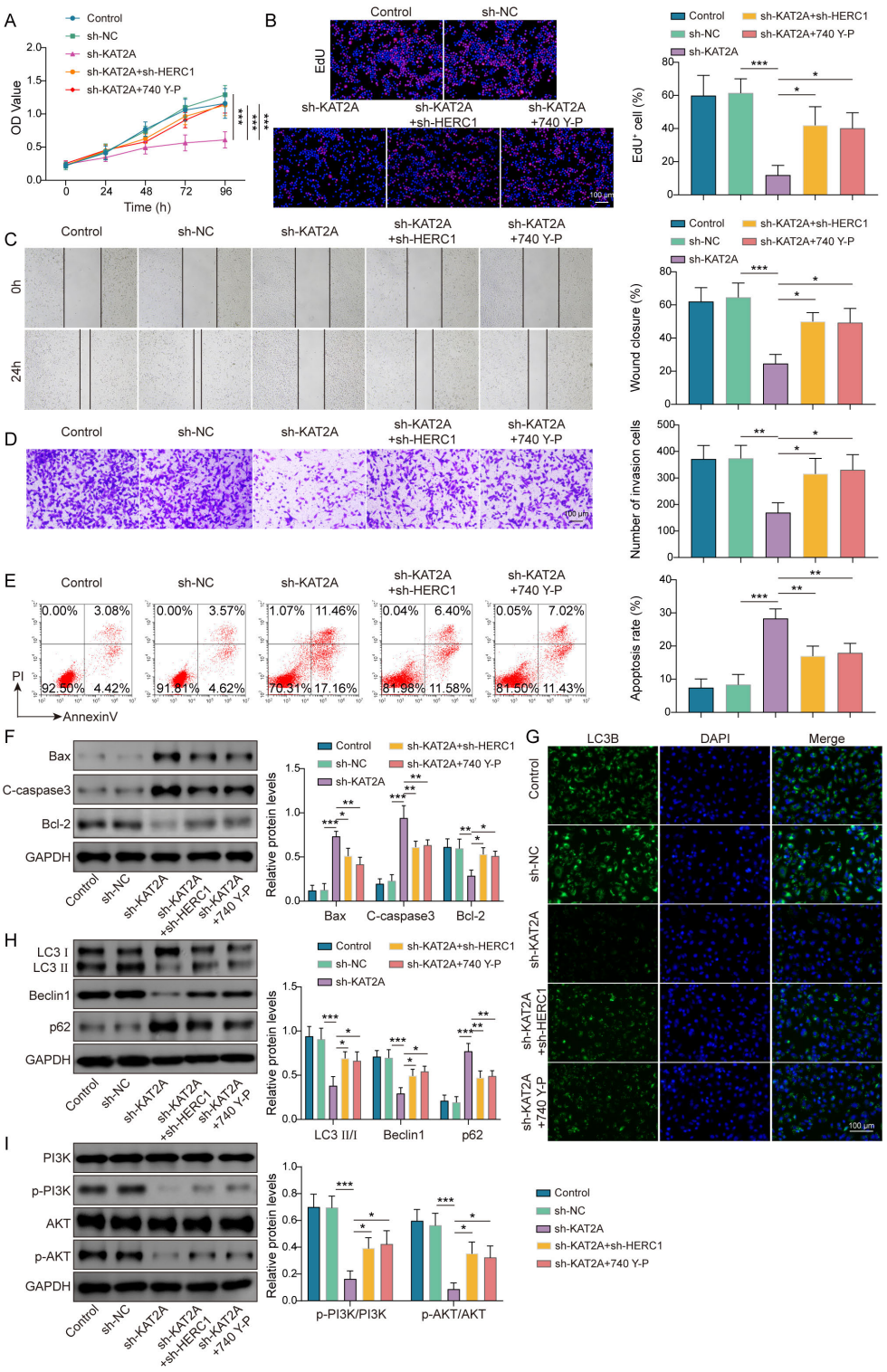

Figure 6. HERC1 repressed autophagy and proliferation of gemcitabine-resistant A549 cells by inactivating the PI3K/AKT signaling axis through KAT2A. A549/R cells were transfected with sh-KAT2A with/without sh-HERC1 or treatment with PI3K activator 740 Y-P. A) Assessment of cell viability by CCK-8 assay. B) EdU staining for cell proliferation. C) Wound healing assay was performed to assess the migratory ability of cells. D) Transwell assay was performed to assess the invasive ability of cells. E) The rate of apoptotic cells was calculated using flow cytometry. F) Protein levels of C-caspase3, Bax, and Bcl-2 in A549/R cells were evaluated by western blot. G) LC3B level was observed by immunofluorescence. H) LC3II/I, Beclin1, and p62 were quantified by western blot. I) The phosphorylation levels of PI3K and AKT were assessed using western blot, n=3. Data were expressed as mean ± SD. *p<0.05, **p<0.01, ***p<0.001

gemcitabine alone (Figures 7A–7C). Furthermore, the proportion of Ki-67-positive cells was obviously decreased by HERC1 upregulation or gemcitabine, which was further reduced by their combination (Figure 7D). Western blot analyses demonstrated that HERC1 was successfully upregulated by oe-HERC1 transfection in the xenograft tumor model with/without gemcitabine administration (Figure 7E). Importantly, the elevation of HERC1 or gemcitabine reduced LC3II/I but promoted p62 expression in tumor tissues, which was enhanced by the combination of upregulating HERC1 (Figure 7F). These findings illustrated that HERC1 upregulation enhanced the sensitivity of lung cancer mice to gemcitabine through mitigating autophagy.

Discussion

Chemoresistance to gemcitabine remains a significant challenge for lung cancer treatment. Autophagy promotes survival and proliferation in drug-resistant cells [28], but its regulatory mechanisms are not fully understood. Our study identified HERC1 as a pivotal regulator of autophagy and gemcitabine resistance. We first demonstrated that HERC1 alleviated gemcitabine resistance by suppressing PI3K/AKT-mediated autophagy through KAT2A ubiquitination in lung cancer.

Accumulating evidence indicates that autophagy contributes to chemoresistance in various cancers. For instance, the long non-coding RNA plasmacytoma variant translocation 1 (lncRNA PVT1) and Troponin C1, Cardiac Type (TNNC1) overexpression have been shown to aggravate gemcitabine resistance via autophagy activation in pancreatic cancer and non-small cell lung cancer (NSCLC) [29, 30]. Notably, autophagy levels were decreased in gemcitabine-resistant CL1-0 lung cancer cells compared to the parental CL1-0 cells [31], possibly because autophagy is induced in parental cells upon gemcitabine treatment to trigger cell death, while resistant cells have adapted to persistent drug-induced stress by maintaining a lower but sustained basal

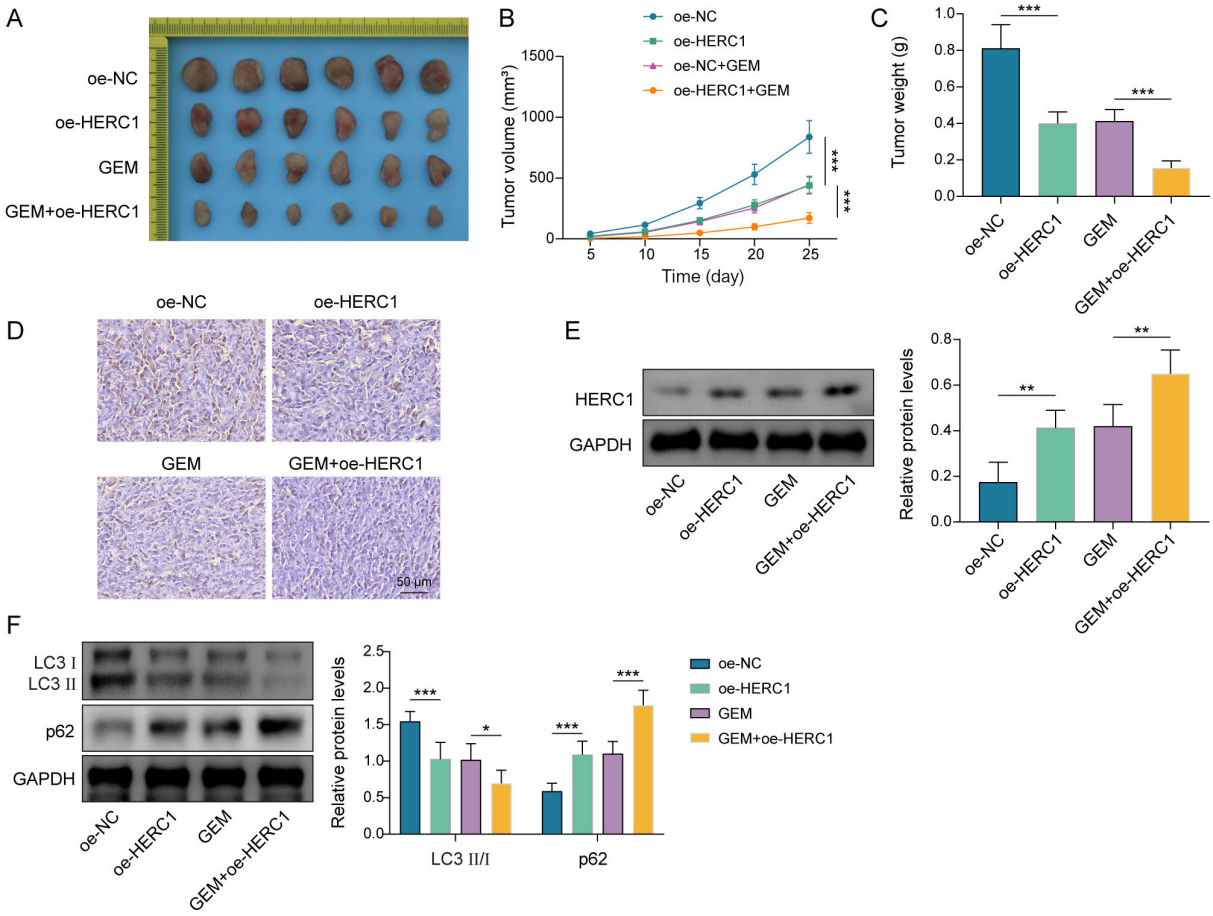

Figure 7. HERC1 overexpression enhanced gemcitabine sensitivity by suppressing autophagy in the xenograft tumor model. A mouse xenograft tumor model was established by subcutaneous transplantation of A549 cells transfected with stable oe-HERC1 or oe-NC, and the mice were intraperitoneally administered 50 mg/kg/day gemcitabine. A–C) Tumor volume and weight were evaluated. D) The proportion of Ki-67-positive cells in tumor tissues was assessed by immunohistochemistry. E) HERC1 protein was detected by western blot. F) LC3II/I and p62 in tumor tissues were determined by western blot, n=6. Data were expressed as mean ± SD. *p<0.05, **p<0.01, ***p<0.001

level of autophagy. In accordance with this, our results revealed that HERC1 overexpression repressed autophagy in both gemcitabine-resistant A549/R and parental A549 cells, as well as H1299 cells. Furthermore, studies have shown that in lung cancer, knockdown of methyltransferase-like 3 (METTL3) inhibited autophagy in doxorubicin-resistant H69 cells [32], while in H157 cells, depletion of Sirtuin 7 (SIRT7) enhanced gemcitabine sensitivity by suppressing autophagy [33]. These findings collectively suggested that in various lung cancer cell lines, whether resistant to chemotherapeutic agents, autophagy activation contributes to the development of chemoresistance. Our data identified HERC1 as a tumor suppressor, consistent with previous findings that show HERC1 inhibits lung adenocarcinoma cell proliferation by promoting ferroptosis [9] and activating autophagy in fibroblasts [11]. Importantly, we found that HERC1 was downregulated in gemcitabine-resistant lung cancer, and its upregulation reversed gemcitabine resistance by suppressing autophagy.

Recent advances have highlighted the role of ubiquitination in modulating protein activity through proteasomal degradation in cancers. For instance, ubiquitination of glutathione peroxidase 4 (GPX4) by bufotalin triggered ferroptosis in NSCLC [34], and tripartite motif containing 3 (TRIM3) promoted solute carrier family 7-member 11 (SLC7A11) degradation to inhibit NSCLC tumorigenesis [35]. We found that HERC1 promoted ubiquitin-mediated degradation of KAT2A in gemcitabine-resistant lung cancer cells, which was increased in lung cancer and correlated with poor prognosis. Consistently, high expression of KAT2A predicted poor survival outcomes for patients with renal cell carcinoma [36]. KAT2A knockdown strengthened abiraterone sensitivity in prostate cancer [37] and partially reduced SF3B4-induced tumorigenesis in lung adenocarcinoma [15]. Our results suggested that HERC1 enhanced gemcitabine sensitivity by inhibiting autophagy via promoting KAT2A degradation in A549/R cells.

Activation of the PI3K/AKT signaling axis is associated with chemoresistance in lung cancer [38]. For example, PI3K/AKT/NF-κB hyperactivation enhanced gemcitabine resistance in lung cancer [39], whereas ononin, combined with paclitaxel, suppressed NSCLC proliferation via inhibition of the PI3K/Akt pathways [40]. We elucidated the novel role of KAT2A in activating PI3K/AKT signaling through PIK3CB lysine acetylation. PIK3CB promoted tumorigenesis in esophageal squamous cell carcinoma via PI3K/AKT/mTOR signaling [27]. Overexpression of KAT2A promoted viability and metastasis in colorectal cancer cells by modulating the histone acetylation of GPX4 [41]. Consistently, we found that KAT2A overexpression activated PI3K/AKT signaling through PIK3CB lysine acetylation in lung cancer cells. Moreover, HERC1 repressed autophagy and proliferation of gemcitabine-resistant lung cancer cells by inactivating PIK3CB-mediated PI3K/AKT signaling through KAT2A.

In conclusion, this study investigated the role of HERC1 and its functional mechanism in gemcitabine resistance of lung cancer. Overexpression of HERC1 repressed autophagy by inactivating PIK3CB-mediated PI3K/AKT signaling via KAT2A ubiquitination, thereby reducing the resistance of lung cancer cells to gemcitabine. Our work might offer a promising new clinical target for gemcitabine-resistant lung cancer. However, this study has several limitations. Although HERC1 shows potential as a therapeutic target, its clinical applicability remains to be fully validated. Secondly, HERC1 may affect gemcitabine resistance by modulating other downstream targets or intersecting with alternative signaling pathways. This will also be the research focus of our subsequent studies.

Supplementary information is are available in the online version of the paper.

Acknowledgments: This work was supported by Wu Jieping Medical Foundation (320.6750.2020-10-75).

References

[1] GUO L, ZHU C, CAI L, ZHANG X, FANG Y et al. Global burden of lung cancer in 2022 and projected burden in 2050. Chin Med J (Engl) 2024; 137: 2577–2582. https://doi.org/10.1097/CM9.0000000000003268

[2] ZHANG Y, VACCARELLA S, MORGAN E, LI M, ETXEBERRIA J et al. Global variations in lung cancer incidence by histological subtype in 2020: a population-based study. Lancet Oncol 2023; 24: 1206–1218. https://doi.org/10.1016/S1470-2045(23)00444-8

[3] WU HM, SHAO LJ, JIANG ZF, LIU RY. Gemcitabine-Induced Autophagy Protects Human Lung Cancer Cells from Apoptotic Death. Lung 2016; 194: 959–966. https://doi.org/10.1007/s00408-016-9936-6

[4] LI X, ZHOU Y, LI Y, YANG L, MA Y et al. Autophagy: A novel mechanism of chemoresistance in cancers. Biomed Pharmacother 2019; 119: 109415. https://doi.org/10.1016/j.biopha.2019.109415

[5] MA K, LI S, HUO X, GUO M, DU X et al. Exploring the mechanism of cisplatin resistance by transcriptome sequencing and reversing the chemoresistance by autophagy inhibition in small cell lung cancer. Biochem Biophys Res Commun 2020; 533: 474–480. https://doi.org/10.1016/j.bbrc.2020.09.023

[6] MAO X, SETHI G, ZHANG Z, WANG Q. The Emerging Roles of the HERC Ubiquitin Ligases in Cancer. Curr Pharm Des 2018; 24: 1676–1681. https://doi.org/10.2174/1381612824666180528081024

[7] ROSSI FA, CALVO ROITBERG EH, ENRIQUÉ STEINBERG JH, JOSHI MU, ESPINOSA JM et al. HERC1 Regulates Breast Cancer Cells Migration and Invasion. Cancers (Basel) 2021; 13: 1309. https://doi.org/10.3390/cancers13061309

[8] ZHANG Y, CHEN Y, MOU H, HUANG Q, JIAN C et al. Synergistic induction of ferroptosis by targeting HERC1-NCOA4 axis to enhance the photodynamic sensitivity of osteosarcoma. Redox Biol 2024; 76: 103328. https://doi.org/10.1016/j.redox.2024.103328

[9] YE F, XU Y, ZHU X, DING Q, WANG Y et al. The mechanism of E3 ubiquitin ligase HERC1 regulating ferroptosis in lung adenocarcinoma cells. Cancer Genet 2025; 292–293: 92–99. https://doi.org/10.1016/j.cancergen.2025.02.001

[10] JANKOVIC M, POON WWL, GONZALES-LOSADA C, VAZQUEZ GG, SHARIF-ASKARI B et al. The E3 ubiquitin ligase Herc1 modulates the response to nucleoside analogs in acute myeloid leukemia. Blood Adv 2024; 8: 5315–5329. https://doi.org/10.1182/bloodadvances.2023011540

[11] SCHWARZ JM, PEDRAZZA L, STENZEL W, ROSA JL, SCHUELKE M et al. A new homozygous HERC1 gain-of-function variant in MDFPMR syndrome leads to mTORC1 hyperactivation and reduced autophagy during cell catabolism. Mol Genet Metab 2020; 131: 126–134. https://doi.org/10.1016/j.ymgme.2020.08.008

[12] PÉREZ-CASTRO M, HERNÁNDEZ-RASCO F, ALONSO-BELLIDO IM, LETRÁN-SÁNCHEZ MS, PÉREZ-VILLEGAS EM et al. HERC1 E3 Ubiquitin Ligase Is Necessary for Autophagy Processes and for the Maintenance and Homeostasis of Vesicles in Motor Nerve Terminals, but Not for Proteasomal Activity. Int J Mol Sci 2025; 26: 793. https://doi.org/10.3390/ijms26020793

[13] JIN JO, PURANIK N, BUI QT, YADAV D, LEE PC. The Ubiquitin System: An Emerging Therapeutic Target for Lung Cancer. Int J Mol Sci 2021; 22: 9629. https://doi.org/10.3390/ijms22179629

[14] BONDY-CHORNEY E, DENONCOURT A, SAI Y, DOWNEY M. Nonhistone targets of KAT2A and KAT2B implicated in cancer biology. Biochem Cell Biol 2019; 97: 30–45. https://doi.org/10.1139/bcb-2017-0297

[15] QU A, HAN B, HUA M, WANG C, LI T. SF3B4 downregulation restrains lung adenocarcinoma tumorigenesis via 5' alternative splicing of KAT2A. Sci Rep 2024; 14: 30. https://doi.org/10.1038/s41598-023-50606-2

[16] IKSEN, POTHONGSRISIT S, PONGRAKHANANON V. Targeting the PI3K/AKT/mTOR Signaling Pathway in Lung Cancer: An Update Regarding Potential Drugs and Natural Products. Molecules 2021; 26: 4100. https://doi.org/10.3390/molecules26134100

[17] TUYA N, WANG Y, TONG L, GAO W, YU R et al. Trichosanthin enhances the antitumor effect of gemcitabine in non-small cell lung cancer via inhibition of the PI3K/AKT pathway. Exp Ther Med 2017; 14: 5767–5772. https://doi.org/10.3892/etm.2017.5286

[18] XU Z, HAN X, OU D, LIU T, LI Z et al. Targeting PI3K/AKT/mTOR-mediated autophagy for tumor therapy. Appl Microbiol Biotechnol 2020; 104: 575–587. https://doi.org/10.1007/s00253-019-10257-8

[19] TIAN Z, TAN Y, LIN X, SU M, PAN L et al. Arsenic trioxide sensitizes pancreatic cancer cells to gemcitabine through downregulation of the TIMP1/PI3K/AKT/mTOR axis. Transl Res 2023; 255: 66–76. https://doi.org/10.1016/j.trsl.2022.11.007

[20] CHENG G, LI L, LI Q, LIAN S, CHU H et al. β-elemene suppresses tumor metabolism and stem cell-like properties of non-small cell lung cancer cells by regulating PI3K/AKT/mTOR signaling. Am J Cancer Res 2022; 12: 1535–1555.

[21] LIN Z, ZHOU P, VON GISE A, GU F, MA Q et al. Pi3k-cb links Hippo-YAP and PI3K-AKT signaling pathways to promote cardiomyocyte proliferation and survival. Circ Res 2015; 116: 35–45. https://doi.org/10.1161/CIRCRESAHA.115.304457

[22] CHEN H, MEI L, ZHOU L, SHEN X, GUO C et al. PTEN restoration and PIK3CB knockdown synergistically suppress glioblastoma growth in vitro and in xenografts. J Neurooncol 2011; 104: 155–167. https://doi.org/10.1007/s11060-010-0492-2

[23] TANG Z, KANG B, LI C, CHEN T, ZHANG Z. GEPIA2: an enhanced web server for large-scale expression profiling and interactive analysis. Nucleic Acids Res 2019; 47: W556–W560. https://doi.org/10.1093/nar/gkz430

[24] LI T, FAN J, WANG B, TRAUGH N, CHEN Q et al. TIMER: A Web Server for Comprehensive Analysis of Tumor-Infiltrating Immune Cells. Cancer Res 2017; 77: e108–e110. https://doi.org/10.1158/0008-5472.CAN-17-0307

[25] GYŐRFFY B. Transcriptome-level discovery of survival-associated biomarkers and therapy targets in non-small-cell lung cancer. Br J Pharmacol 2024; 181: 362–374. https://doi.org/10.1111/bph.16257

[26] MA X, FU T, KE ZY, DU SL, WANG XC et al. MiR-17- 5p/RRM2 regulated gemcitabine resistance in lung cancer A549 cells. Cell Cycle 2023; 22: 1367-1379. https://doi.org/10.1080/15384101.2023.2207247

[27] XU W, WANG Z, ZHANG Z, XU J, JIANG Y. PIK3CB promotes oesophageal cancer proliferation through the PI3K/AKT/mTOR signalling axis. Cell Biol Int 2022; 46: 1399–1408. https://doi.org/10.1002/cbin.11847

[28] SMITH AG, MACLEOD KF. Autophagy, cancer stem cells and drug resistance. J Pathol. 2019; 247: 708–718. https://doi.org/10.1002/path.5222

[29] ZHOU C, YI C, YI Y, QIN W, YAN Y et al. LncRNA PVT1 promotes gemcitabine resistance of pancreatic cancer via activating Wnt/β-catenin and autophagy pathway through modulating the miR-619-5p/Pygo2 and miR-619-5p/ATG14 axes. Mol Cancer 2020; 19: 118. https://doi.org/10.1186/s12943-020-01237-y

[30] YE X, XIE G, LIU Z, TANG J, CUI M et al. TNNC1 Reduced Gemcitabine Sensitivity of Nonsmall-Cell Lung Cancer by Increasing Autophagy. Med Sci Monit 2020; 26: e922703. https://doi.org/10.12659/MSM.922703

[31] CHIU CH, RAMESH S, LIAO PH, KUO WW, CHEN MC et al. Phosphorylation of Bcl-2 by JNK confers gemcitabine resistance in lung cancer cells by reducing autophagy-mediated cell death. Environ Toxicol 2023; 38: 2121–2131. https://doi.org/10.1002/tox.23836

[32] SUN Y, SHEN W, HU S, LYU Q, WANG Q et al. METTL3 promotes chemoresistance in small cell lung cancer by inducing mitophagy. J Exp Clin Cancer Res 2023; 42: 65. https://doi.org/10.1186/s13046-023-02638-9

[33] JIANG Y, HAN Z, WANG Y, HAO W. Depletion of SIRT7 sensitizes human non-small cell lung cancer cells to gemcitabine therapy by inhibiting autophagy. Biochem Biophys Res Commun 2018; 506: 266–271. https://doi.org/10.1016/j.bbrc.2018.10.089

[34] ZHANG W, JIANG B, LIU Y, XU L, WAN M. Bufotalin induces ferroptosis in non-small cell lung cancer cells by facilitating the ubiquitination and degradation of GPX4. Free Radic Biol Med 2022; 180: 75–84. https://doi.org/10.1016/j.freeradbiomed.2022.01.009

[35] WANG Z, SHEN N, WANG Z, YU L, YANG S et al. TRIM3 facilitates ferroptosis in non-small cell lung cancer through promoting SLC7A11/xCT K11-linked ubiquitination and degradation. Cell Death Differ 2024; 31: 53–64. https://doi.org/10.1038/s41418-023-01239-5

[36] GUO Y, LIU B, LIU Y, SUN W, GAO W et al. Oncogenic Chromatin Modifier KAT2A Activates MCT1 to Drive the Glycolytic Process and Tumor Progression in Renal Cell Carcinoma. Front Cell Dev Biol 2021; 9: 690796. https://doi.org/10.3389/fcell.2021.690796

[37] LU D, SONG Y, YU Y, WANG D, LIU B et al. KAT2A-mediated AR translocation into nucleus promotes abiraterone-resistance in castration-resistant prostate cancer. Cell Death Dis 2021; 12: 787. https://doi.org/10.1038/s41419-021-04077-w

[38] JIN Y, CHEN Y, TANG H, HU X, HUBERT SM et al. Activation of PI3K/AKT Pathway Is a Potential Mechanism of Treatment Resistance in Small Cell Lung Cancer. Clin Cancer Res 2022; 28: 526–539. https://doi.org/10.1158/1078-0432.CCR-21-1943

[39] CHIU CH, LIN YJ, RAMESH S, KUO WW, CHEN MC et al. Gemcitabine resistance in non-small cell lung cancer is mediated through activation of the PI3K/AKT/NF-κB pathway and suppression of ERK signaling by reactive oxygen species. J Biochem Mol Toxicol 2023; 37: e23497. https://doi.org/10.1002/jbt.23497

[40] GONG G, GANESAN K, XIONG Q, ZHENG Y. Antitumor Effects of Ononin by Modulation of Apoptosis in Non-Small-Cell Lung Cancer through Inhibiting PI3K/Akt/mTOR Pathway. Oxid Med Cell Longev 2022; 2022: 5122448. https://doi.org/10.1155/2022/5122448

[41] XU Z, WANG X, YU P, ZHANG Y, HUANG L et al. Lysine acetyltransferase KAT2A modulates ferroptosis during colorectal cancer development. Scand J Gastroenterol 2024; 59: 437–444. https://doi.org/10.1080/00365521.2023.2301331

https://doi.org/10.4149/neo_2025_250620N274

HERC1 attenuates gemcitabine resistance of lung cancer cells by inhibiting autophagy through KAT2A ubiquitination

Yanhong WEI, Guanghui TIAN, Zhaohui TANG, Sijuan DING, Zhangwen TANG, Pengfei LUO*

Supplementary Information

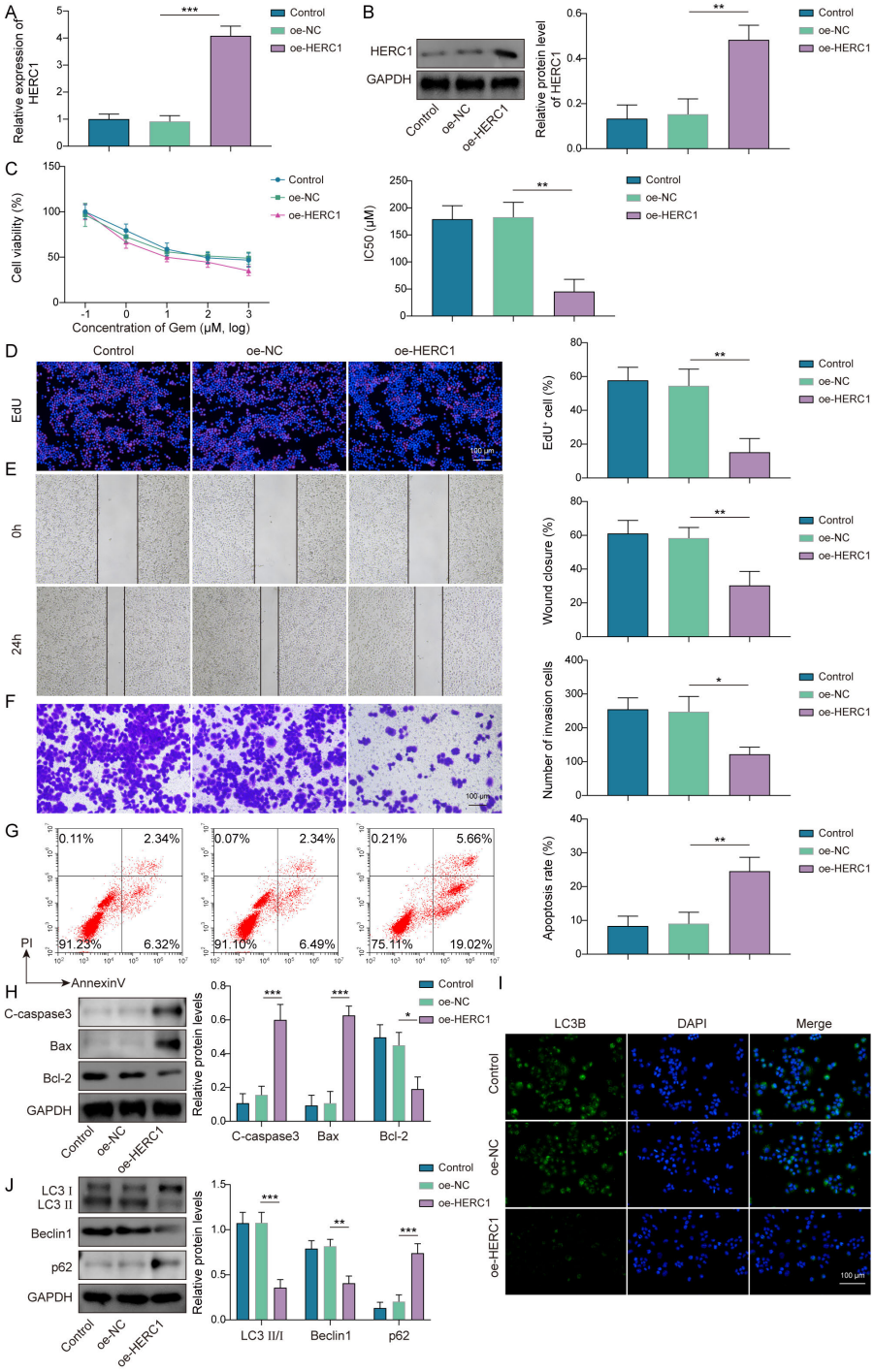

Supplementary Figure S1. HERC1 overexpression inhibited autophagy and proliferation of gemcitabine-resistant H1299 cells. A) H1299/R cells were transfected with overexpressing HERC1 or negative control. qRT-PCR assay was conducted to calculate HERC1 expression in H1299/R cells. B) HERC1 protein expression was quantified using western blot. C) H1299/R cells were treated with gemcitabine at different concentrations (0.1; 1; 10; 100; 1,000 μM). Cell viability was evaluated by CCK-8 assay. A549/R cells were treated with oe-HERC1. D) Cell proliferation was evaluated by EdU staining. E) Wound healing assay was applied to assess the migratory ability of cells. F) Transwell assay was performed to assess the invasive ability of cells. G) Cell apoptosis rate was detected by flow cytometry. H) Protein levels of C-caspase3, Bax and Bcl-2 were examined by western blot. I) The expression level of LC3B was detected by immunofluorescence. J) LC3II/I, Beclin1 and p62 were quantified by western blot. N=3. Data was expressed as mean±SD. *p<0.05, **p<0.01, ***p<0.001

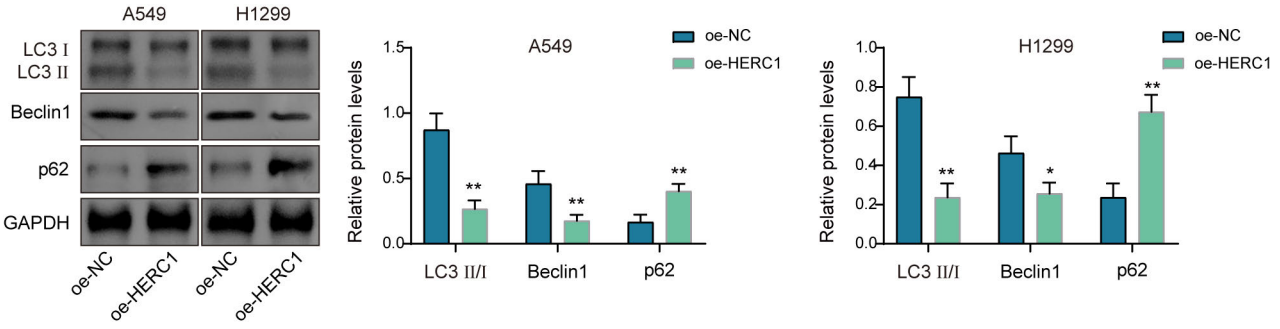

Supplementary Figure S2. HERC1 overexpression inhibited autophagy of parental A549 and H1299 cells. A549 and H1299 cells were transfected with oe-HERC1 or oe-NC. Protein levels of LC3II/I, Beclin1 and p62 were examined by western blot. N=3. Data was expressed as mean±SD. *p<0.05, **p<0.01, ***p<0.001

Supplementary Table S1. Association between HECR1 expression and clinicopathological characteristics

Clinical characteristics	HECR1			p-value
	N=30	High	Low	
Gender				0.4621
Male	13	5	8	
Female	17	10	7	
Age (years)				0.7152
<55	14	6	8	
≥55	16	9	7	
N Stage				
N0	7	5	2	0.0603
N1	12	8	4	
N2	9	2	7	
N3	2	0	2	
Smoking				
Yes	12	5	7	0.7104
No	18	10	8	